International Symposium
On Turbulence and Shear Flow
Phenomena (TSFP-8)
August 28 - 30, 2013 Poitiers, France

A NOTE ON LOCAL ISOTROPY CRITERIA IN SHEAR FLOWS WITH COHERENT MOTION

Thiesset Fabien
School of Engineering,
University of Newcastle, Australia

Danaila Luminita
CORIA, UMR 6614,
University of Rouen, France

Antonia Robert
School of Engineering,
University of Newcastle, Australia

ABSTRACT

Whilst Local Isotropy (LI) is widely used, it is also necessary to test its validity, especially in shear flows, characterized by large-scale anisotropy. Important questions are whether the small scales are isotropic and how their properties depend on large-scale parameters (mean shear, the shear induced by a coherent motion, the Reynolds number etc.). We focus on two families of LI tests:

i) classical, kinematic tests, in which time-averages are compared to their isotropic values. The large-scale parameters do not appear explicitly. We only use here one example of such tests.

ii) Phenomenological tests, which explicitly account for the large-scale strain, as well as its associated dynamics. In flows populated by coherent motions in which phase-averages are pertinent for describing the flow dynamics, we propose a Local Isotropy (LI) criterion based on the intensity of the turbulent strain rate at a given scale $\vec{r}$ and a particular phase ϕ, $s_\phi(\vec{r},\phi)$. The formulation is the following: "If LI were to be valid at a vectorial scale $\vec{r}$ and a phase ϕ, then the intensity of the turbulent strain rate $s_\phi(\vec{r},\phi)$ should prevail over the combined effect of the mean shear $\overline{S}$ and of the shear $\widetilde{S}$ associated with the coherent motion". The mathematical expression of $s_\phi(\vec{r},\phi)$ depends on the Laplacian of the total kinetic energy second-order structure function. Therefore, the proposed expression allows the eventual anisotropy to be taken into account. The new LI criterion is used together with data taken in the intermediate wake behind a circular cylinder. It is highlighted that (i) when $\overline{S}+\widetilde{S}$ is important, LI only holds for scales smaller than the Taylor microscale (ii) when $\overline{S}+\widetilde{S}$ is small, the domain in which LI is valid extends up to the largest scales.

INTRODUCTION

Local isotropy (LI) is seemingly one of the most important hypotheses on small-scale statistics. LI was first enunciated by Kolmogorov (1941), and further utilized and sometimes tested, in most of the laboratory flows. From the analytical viewpoint, LI leads to simplified expressions of e.g. the total kinetic energy, the dissipation rate of kinetic energy or scalar variance, structure functions at a given scale. Simple expressions of statistics are useful for the experimentalists, because of the limited possibilities to measure all the velocity components, as well as their spatial distribution.

Although LI is extensively used, it is nonetheless necessary to test its validity, especially in shear flows, characterized by large-scale anisotropy. Important questions are whether the small scales are isotropic and if there is a clear dependence of their statistics on large-scale parameters (mean shear $\overline{S}$, the shear induced by a coherent motion $\widetilde{S}$, the Reynolds number etc.).

Using a compilation of experimental and numerical data, Schumacher *et al.* (2003) showed that LI prevails for small values of the ratio $\overline{S}/R_\lambda$ (R_λ is the Taylor microscale Reynolds number). One should expect that the magnitude of the shear will play some role in determining how high an R_λ is required for LI to prevail. Whereas the conclusion of Schumacher *et al.* (2003) is optimistic quid the restoration of LI, the analytical study of Durbin & Speziale (1991) demonstrated that small scales cannot be isotropic in shear flows, independently of the values of R_λ and $\overline{S}$. From a general viewpoint, the assessment of LI can only be done through specific criteria and a definitive conclusion about the validity of LI is unlikely to be realistic.

The aim of this study is to understand how, in the context of shear flows, the anisotropy propagates across the scales from the largest to the smallest, how it evolves down the scales and finally, what the degree of anisotropy is at any given scale. To this end, we propose a phenomenological LI criterion based on the intensity of the turbulent strain rate at a given scale r.

As a first step in answering the question of what the isotropy level is at any particular scale, we consider flows populated by a single-scale, persistent coherent motion (hereafter, CM). A good candidate is the cylinder wake flow, and this study focuses entirely on this flow. The other advantage of investigating the wake flow is that it allows to invoke phase averages. The latter operation results in a dependence of any statistical quantities on the phase ϕ characterizing the temporal dynamics of the CM.

We focus on two families of LI tests:

i) classical, kinematic tests, in which time-averages are compared to their isotropic values. The large-scale parameters (shear) does not appear explicitly. We only use here one example of such tests.

ii) Phenomenological tests, which explicitly account for the

large-scale strain rate, as well as its associated dynamics.

PHENOMENOLOGICAL LI TESTS. ANALYTICAL CONSIDERATIONS

The formulation of the LI criterion is the following (Thiesset *et al.* (2013)): "For LI to be valid at a vectorial scale $\vec{r}$ and a phase ϕ, then the intensity of the strain rate at that scale due to any larger scale must be much larger than the combined effect of the mean shear $\overline{S}$ and of $\widetilde{S}$, the shear associated with the coherent motion". Identically and in the spirit of Corrsin (1958), LI requires the time scale associated with s_ϕ to be smaller than that due to the sum $\overline{S}+\widetilde{S}$.

Mathematically, this can be expressed in terms of the following inequality

$$s_\phi(\vec{r},\phi) \gg \widetilde{S}_\phi, \tag{1}$$

with

$$\widetilde{S}_\phi = |\langle S \rangle|, \tag{2}$$

where $\langle . \rangle$ denotes phase averaging, $|\langle S \rangle| = \left|\overline{S}+\widetilde{S}\right|$ is the absolute value of the phase averaged strain rate $S = \frac{1}{2}\left(\frac{\partial U_i}{\partial x_j}+\frac{\partial U_j}{\partial x_i}\right)$ and $s_\phi(\vec{r},\phi)$ is the phase-averaged strain intensity at the scale $\vec{r}$ and the phase ϕ. Repeated indices indicate summation.

By integrating over all values of ϕ, the classical time averaged quantities are obtained (here denoted by overbars). Under these conditions, the latter inequality reads

$$s(\vec{r}) \gg \widetilde{S}_t, \tag{3}$$

where $s(\vec{r})$ is the time-averaged strain intensity at the scale $\vec{r}$, and $S_t = \overline{\widetilde{S_\phi}}$.

The next step is to propose adequate expressions for the turbulent strain rate $s(\vec{r})$ and $s_\phi(\vec{r},\phi)$. Starting from the definition of the strain tensor $\Sigma = \nabla_{\vec{x}}\vec{u}$, we need to further define the tensor $\mathscr{S}\Sigma$ characterizing the strain at a scale $\vec{r}$ associated with all the larger scales (Mouri & Hori (2010), Danaila *et al.* (2012)), *i.e.* the quantity $\mathscr{S}\Sigma(\vec{r}) \equiv \nabla_{\vec{x}^+}\vec{u}^+ + \nabla_{\vec{x}}\vec{u}$, with $\vec{x}^+ = \vec{x}+\vec{r}$. By considering the two frames to be independent (Monin & Yaglom (2007)), with $\overline{\vec{U}}$ identical in the two frames and by invoking the same decomposition as proposed by e.g. Hill (2002) the final result is

$$\mathscr{S}\Sigma(\vec{r}) = \nabla_{\vec{r}}\Delta\vec{u}. \tag{4}$$

Therefore, as far as the turbulent field is concerned, the turbulent strain intensity, which is the norm of $\mathscr{S}\Sigma$, may be defined as follows

$$s(\vec{r}) = \overline{(\nabla_{\vec{r}}\Delta\vec{u})^2}^{1/2}. \tag{5}$$

After some calculations and by supposing that $\overline{\Delta u_j \frac{\partial^2}{\partial r_k^2}\Delta u_j} \approx 0$ (which is strictly true for $\vec{r}\to 0$), the final expression of $s(\vec{r})$ for turbulent flows in which time-averages are adequate, is the following

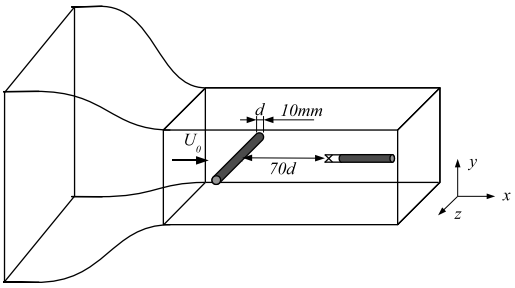

Figure 1. Sketch of the experimental apparatus.

$$s(\vec{r}) = \left(\frac{1}{2}\mathscr{L}\overline{(\Delta u_i)^2}\right)^{1/2}(\vec{r}), \tag{6}$$

where $\mathscr{L}$ represents the Laplacian operator. In flows populated by CM, in which phase-averages are more useful, the intensity of the strain depends on both $\vec{r}$ and the phase ϕ, and it reads (Thiesset *et al.* (2013))

$$s_\phi(\vec{r},\phi) = \left(\frac{1}{2}\mathscr{L}\left\langle(\Delta u_i)^2\right\rangle\right)^{1/2}(\vec{r},\phi). \tag{7}$$

Calculating the Laplacian of these functions requires estimates of the velocity field in several planes, such as provided by PIV (Particle Image Velocimetry), or, preferably, numerical simulations.

It is important to note that, for LI, the Laplacian can be expressed in spherical coordinates as follows

$$s_\phi(r,\phi) = \left(\frac{1}{r}\frac{\partial}{\partial r}\left\langle(\Delta u_i)^2\right\rangle + \frac{1}{2}\frac{\partial^2}{\partial r^2}\left\langle(\Delta u_i)^2\right\rangle\right)^{1/2}(r,\phi). \tag{8}$$

The first term on the right side of Eq. (8) has already been proposed by Danaila *et al.* (2012). This expression will be used later in this paper in order to infer s_ϕ and investigate phenomenological LI tests involving phase averages.

EXPERIMENTS

Measurements were performed at the CORIA, University of Rouen, in a circular cylinder wake. The wind tunnel is of the recirculating type with a residual turbulence level smaller than 0.2 %. The test section is 0.4×0.4 m^2 and 2.5m long and the mean pressure gradient was adjusted to zero. The circular cylinder of diameter $d = 10mm$ was placed horizontally, downstream the contraction, spanning the whole test section. The upstream velocity was $U_0 = 6.5m.s^{-1}$ corresponding to a Reynolds number based on the cylinder diameter of 4333 and a Taylor microscale Reynolds number of $R_\lambda \equiv \frac{u'\lambda_u}{\nu} = 70$. Here, u' is the root mean squared of the longitudinal velocity component u, λ_u is the Taylor microscale and ν is the kinematic viscosity of the air. Measurements were made at $70d$ downstream of the cylinder and for transverse positions varying between $y = 0$ and $y = 5d$ (Fig. 1).

Only the streamwise and the transverse velocity component u and v were measured. The X-wire probe (Dantec

55P51) was calibrated using a look-up table technique, with velocity increments of 1 m/s and angle increments of 5^0. The hot wires were operated by a Dantec constant temperature bridge, with an overheat ratio of 0.6. Voltage signals were passed through gain circuits (SRS SIM983) and low pass filtered (SRS SIM965) at a frequency close to the Kolmogorov frequency. The air temperature in the wind tunnel is kept constant during calibration and measurements, thus avoiding any systematic errors which may arise from slight variations in the mean temperature on the output characteristics of the hot wires.

Phase-averaged statistics are obtained as follows. The transverse velocity component v is first digitally band-pass filtered at the frequency corresponding to the peak in the v spectrum, using an eighth-order Butterworth filter. The filtering operation is applied to the Fourier transform of v in order to avoid any phase shift. Then, the Hilbert transform h of the filtered signal v_f is obtained and the phase ϕ inferred from the relation $\phi = \arctan\left(\frac{h}{v_f}\right)$. Finally, the phase is divided into 41 segments and phase-averaged statistics are calculated for each class. The convergence of statistics was checked, by reducing the number of classes, and found to be satisfactory. By means of our method, phase-averaged quantities are calculated over the period $[-\pi,\pi]$. As was done by O'Neil & Meneveau (1997), the phase is doubled up to $[-2\pi,2\pi]$ thanks to the periodicity, in order to enhance the visual display.

In Hill (2001), the geometrical space (location $\vec{x}$ in the flow) and the separation space (turbulent scales $\vec{r}$) are made independent by considering the geometrical location specified by the midpoint $\vec{X} = \frac{1}{2}\left(\vec{x}+\vec{x^+}\right)$. The same idea is applied here to phase-conditioned structure functions for which the phase ϕ is defined as the phase at the midpoint $\phi = \phi(\vec{X})$. Therefore, each velocity component is decomposed into a triple contribution from the mean temporal average, the phase-averaged fluctuation and the random/turbulent fluctuation.

RESULTS IN THE WAKE FLOW

One-point statistics

One of the main advantages of using phase averages is that the temporal dynamics associated with the presence of the CM is highlighted. As far as the wake flow is concerned, one generally displays statistics in the (ϕ,y) plane to relate the spatial organization of the kinetic energy with that of the coherent structures. Here, we focus particularly on the coherent strain. The maxima of the total strain rate are noted at phases which are $-\pi/2+2n\pi$ (n is a positive integer), corresponding to the position of the saddle points (Fig. 2). Also illustrated in the same figure are the streamlines of the coherent vortices. The most visible are two of them, rotating clockwise (the upper stream moves from left to right). The centres of these vortices are located at $y/d \approx 1.4$ and phases $\phi = -3\pi/2 \pm 2n\pi$ and correspond to the minimum total strain $\langle S\rangle$. Note that on the wake centerline, the periodicity of the total strain rate is π, whereas it is 2π out of the centerline.

Phase-averaging inescapably leads to a dependence on the phase ϕ, and eventually on the scale r of the flow, as is the case for structure functions at any order.

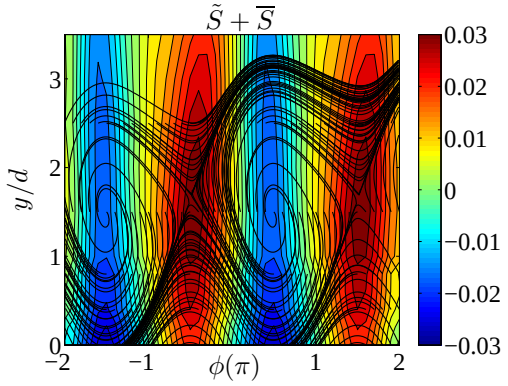

Figure 2. The total strain rate $\langle S\rangle\, d/U_0$ as a function of the phase ϕ and the vertical position in the wake, y/d.

Two-point statistics

Figure 3 represents the phase-averaged second-order structure functions for v normalized by its variance, $\langle(\Delta v)^2\rangle/\overline{v^2}$, as a function of the scale r/λ_u and the phase $\phi(\pi)$ of the coherent motion.

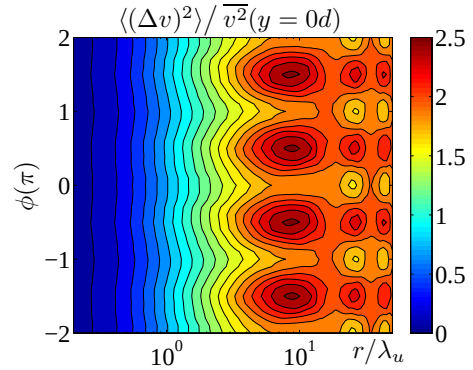

Figure 3. Values of $\langle(\Delta v)^2\rangle(r,\phi)/\overline{v^2}$ as a function of r/λ_u and the phase $\phi(\pi)$ at $y = 0d$ and $R_\lambda \simeq 70$.

The values of the scale-phase second-order structure functions progressively increase as r keeps increasing, and reach a maximum for $r/\lambda_u \approx 9$ (this scale is equal to half the distance between two successive vortices), followed first by a slight decrease and then by a quasi-periodic behaviour for the largest scales. The maxima of $\langle(\Delta v)^2\rangle(r,\phi)/\overline{v^2}$ occur at scales which are multiples of the first maximum. The trend of $\langle(\Delta v)^2\rangle(r,\phi)/\overline{v^2}$ is uniform in ϕ for small scales, consistent with the fact that these scales are not influenced by the coherent motion. At larger scales, where the CM is present, there is a hint of periodicity along the ϕ axis (for $r/\lambda_u \approx 2$), followed by a clear periodicity at scales $r/\lambda_u \approx 9$, as emphasised earlier. At these scales, turbulent fluctuations diminish and the CM is predominant.

The dynamical aspect of $\langle(\Delta v)^2\rangle(r,\phi)$ should be understood in association with the phase variations of the total strain rate, Fig. 2. A careful analysis of this figure reveals that the maxima of $\langle(\Delta v)^2\rangle(r,\phi)/\langle v^2\rangle$ occur at the same phases as the extrema of the total strain rate $\overline{S}+\widetilde{S}$ (i.e. odd multiples of $\pi/2$).

Local Isotropy criterion

LI is first assessed from a kinematic LI test relating phase-conditioned second-order structure functions. In this context, the isotropic relation between second-order structure functions of the longitudinal velocity components and those of the transverse velocity components may be written as

$$\left\langle (\Delta u_\perp)^2 \right\rangle_{iso}(r,\phi) = \left(1 + \frac{r}{2}\frac{\partial}{\partial r}\right)\left\langle (\Delta u)^2 \right\rangle(r,\phi). \quad (9)$$

Note the analogy between (9) and its time-averaged counterpart

$$\overline{(\Delta u_\perp)^2}_{iso}(r) = \left(1 + \frac{r}{2}\frac{\partial}{\partial r}\right)\overline{(\Delta u)^2}, \quad (10)$$

It is obvious that such a criterion for LI at each phase of the motion is much more constraining than its time-averaged counterpart, Eq. (10).

We present results for the ratio $\left\langle (\Delta u_\perp)^2 \right\rangle_{iso}(r,\phi) / \left\langle (\Delta u_\perp)^2 \right\rangle(r,\phi)$, where $\left\langle (\Delta u_\perp)^2 \right\rangle_{iso}$ is given by relation (9). This ratio is illustrated in Fig. 4 on the wake centerline.

The most important remark concerns the positions at which the maximum departure of the ratio from the isotropic value of 1 is observed. There are points for which the value of $\left\langle (\Delta v)^2 \right\rangle_{iso}(r,\phi) / \left\langle (\Delta v)^2 \right\rangle(r,\phi)$ is 0.8. This occurs at phases which are odd multiples of $\pi/2$, for which the absolute value of the total strain rate is maximal, and with scales as large as $\approx 8\lambda_u$. Therefore, by considering the phase-conditioned LI test Eq. (9), the relation between anisotropy and the coherent strain can be emphasized.

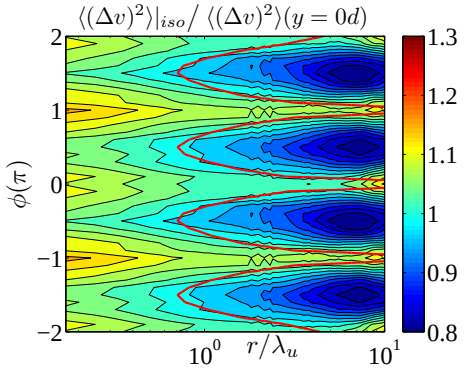

Figure 4. The dependence of $\left\langle (\Delta v)^2 \right\rangle_{iso}(r,\phi) / \left\langle (\Delta v)^2 \right\rangle(r,\phi)$ on r/λ_u and $\phi(\pi)$ at $y/d = 0$ and $R_\lambda \simeq 70$. The red line depicts the scale L_{-1}, representative for the phenomenological LI criterion.

We now turn our attention to the phenomenological LI criterion proposed in this study and thus $s_\phi(r,\phi) \gg \tilde{S}_\phi(\phi)$ is tested against experimental data. Figure 5 depicts $\log_{10}(\tilde{S}_\phi / s_\phi)$ as functions of r/λ_u and the phase ϕ/π at a spatial location $y/d = 0$ at the centerline. A possible statement of the LI criterion is 'LI should hold if $\log_{10}(\tilde{S}_\phi / s_\phi) \leq -1$'. Small values of $\log_{10}(\tilde{S}_\phi / s_\phi)$ occur for small scales, whereas large values (much larger than 10^{-1}), as highlighted by white regions, are found mostly at large scales. The curve for which $\log_{10}(\tilde{S}_\phi / s_\phi) = -1$, i.e. '$L_{-1}$', is represented by dotted lines. This curve separates the region of small values of r (for which LI holds), from the region of large anisotropic scales. As emphasised by this figure, L_{-1} varies between $0.8\lambda_u$ and $8\lambda_u$. The phase for which L_{-1} is minimum is fully correlated with the extremum values of the coherent strain rate $\tilde{S}_\phi$ (Fig. 2) and of the maximum of anisotropy. At the phases for which $\tilde{S}_\phi = 0$, the influence of the coherent motion is absent, so that LI becomes more noticeable and L_{-1} can increase.

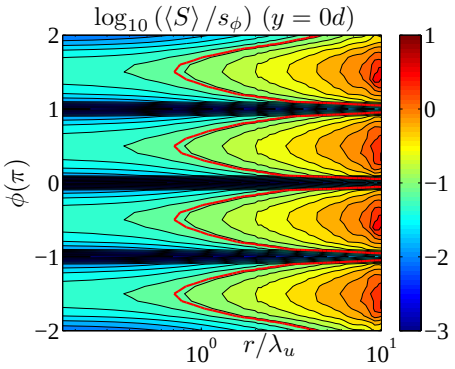

Figure 5. Values of $\log_{10}(\tilde{S}_\phi / s_\phi)$ as functions of r/λ_u and the phase ϕ/π, at $y/d = 0$. The red line represents the scale L_{-1}.

The second similarity hypothesis reads

$$\left\langle (\Delta u_i)^2 \right\rangle \propto r^{2/3} \langle \varepsilon \rangle^{2/3}, \quad (11)$$

so that the strain rate at a given scale which lies in the inertial range

$$s(r,\phi) \propto r^{-2/3} \langle \varepsilon \rangle^{1/3} \quad (12)$$

which is simply the inverse of the Kolmogorov time scale extended to the inertial range. From Eq. (12) yields an analytical expression for L_{-1}

$$L_{-1}(\phi) \propto \sqrt{\frac{\langle \varepsilon \rangle}{|\langle S \rangle|^3}} \quad (13)$$

This expression for L_{-1} is the generalization of the anisotropic scale originally proposed by Corrsin (1958) in which the phase dependence of the coherent motion is explicitly accounted for.

RESULTS IN PRESENCE OF A MEAN SHEAR

We now focus on the sheared region of the flow where the mean shear is not negligible.

Figure 6 represents the phase-averaged second-order structure functions for v normalized by its variance, $\langle (\Delta v)^2 \rangle / \overline{v^2}$, as a function of the scale r/λ_u and the phase $\phi(\pi)$ of the coherent motion, at $y/d = 1.3$. The behaviour of $\langle (\Delta v)^2 \rangle / \overline{v^2}$ at $y/d = 1.3$ is very similar to that on the

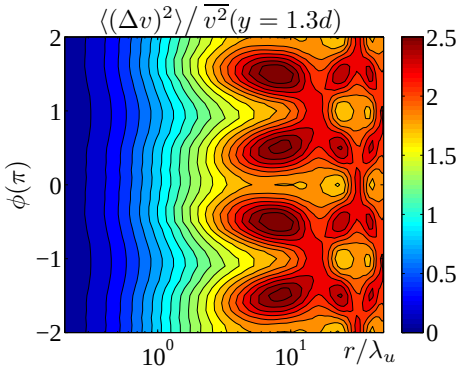

Figure 6. Values of $\langle(\Delta v)^2\rangle(r,\phi)/\overline{v^2}$ as a function of r/λ_u and the phase $\phi(\pi)$ at $y = 1.3d$ and $R_{\lambda_u} \simeq 70$.

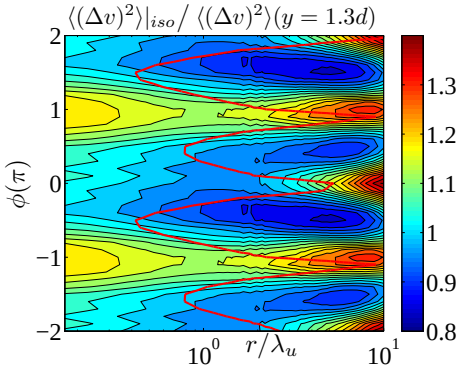

Figure 7. The dependence of $\langle(\Delta v)^2\rangle_{iso}(r,\phi)/\langle(\Delta v)^2\rangle(r,\phi)$ on r/λ_u and $\phi(\pi)$ at $y/d = 1.3$ and $R_\lambda \simeq 70$. The red line represents the scale L_{-1}.

wake centreline. As it was previously noted (Fig. 3), these maxima of $\langle(\Delta v)^2\rangle(r,\phi)/\overline{v^2}$ occur at phases for which $\widetilde{S}$ is extremum, and for $r/\lambda_u \approx 9$. It is worth noting that away from the centreline, the periodicity of these regions is not π, but rather 2π (a complete period of the coherent motion). This behaviour is associated with the fact that for e.g. $\phi(\pi) = 0.5$, $\widetilde{S} < 0$ (see Fig. 2), the total strain rate $\overline{S} + \widetilde{S}$ is smaller than $\overline{S}$, and for these phases, the local strain rate is diminished. On the contrary, at $\phi(\pi) = -0.5$ (and multiples), $\widetilde{S} > 0$ (see Fig. 2), the total strain $\overline{S} + \widetilde{S}$ is larger than $\overline{S}$, and at these phase locations, the local strain is enhanced. For phases associated with $\widetilde{S} > 0$, therefore with a maximal total strain rate, the increase of the ratio $\langle(\Delta v)^2\rangle(r,\phi)/\overline{v^2}$ towards the maximum value of 2.5 is more important and starts at smaller scales ($r/\lambda_u \approx 3$) than for phases where $\widetilde{S} < 0$.

Also presented are results for a LI test from a dynamical viewpoint, i.e. the ratio $\langle(\Delta v)^2\rangle_{iso} / \langle(\Delta v)^2\rangle$. This ratio is illustrated in Fig. 7 at $y/d = 1.3$. If LI holds at a scale r and a phase ϕ, then the ratio $\langle(\Delta v)^2\rangle_{iso} / \langle(\Delta v)^2\rangle$ should be equal to 1. The maximum departure of the ratio from the isotropic value of 1 is associated with phases which are odd multiples of $\pi/2$, for which the absolute value of the total strain rate is maximal, and with scales as large as $\approx 20\lambda_u$. At these scales, the value of $\langle(\Delta v)^2\rangle_{iso} / \langle(\Delta v)^2\rangle$ is 1.3.

Figure 8 depicts $\log_{10}(\tilde{S}_\phi / s_\phi)$ as functions of r/λ_u and the phase ϕ/π, at a spatial location $y/d = 1.3$ away from the

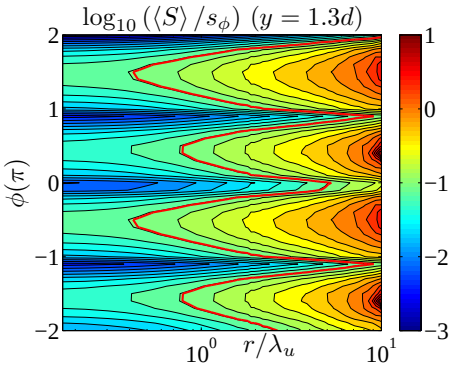

Figure 8. Values of $\log_{10}(\tilde{S}_\phi/s_\phi)$ as functions of r/λ_u and the phase ϕ/π, at $y/d = 1.3$. The red line represents the scale L_{-1}.

centerline. Again, a possible statement of the LI criterion is 'LI should hold if $\log_{10}(\tilde{S}_\phi/s_\phi) \leq -1$'. As in the case of results previously presented at the wake centerline, small values of $\log_{10}(\tilde{S}_\phi/s_\phi)$ occur for small scales, whereas large values (much larger than -1) are found mostly at large scales. The curve for which $\log_{10}(\tilde{S}_\phi/s_\phi) = -1$, i.e. '$L_{-1}$', is represented by red line. This curve separates the region of small values of r (for which LI holds), from the region with large anisotropic scales. As emphasised by this figure, L_{-1} varies between $0.8\lambda_u$ and $8\lambda_u$. Its magnitude is smaller than at the wake centerline, where the mean shear is absent. The phase for which L_{-1} is minimum is fully correlated with the extremum values of the coherent strain rate $\tilde{S}_\phi$ (Fig. 2). At the phases for which $\tilde{S}_\phi = 0$, the influence of the coherent motion is absent, so that LI becomes more noticeable and L_{-1} can increase.

EFFECT OF REYNOLDS NUMBER AND PERSISTING EFFECTS IN THE FAR FIELD

It can be interesting to assess the degree at which LI will be satisfied in the context of large Reynolds numbers shear flows. From Eq. (12), we obtain at an arbitrary scale r

$$s(r)/\overline{\langle\tilde{S}\rangle} \propto R_\lambda^0. \tag{14}$$

Therefore, the amplitude of the turbulent strain rate in the inertial range increases at the same rate as the total strain rate $\overline{S} + \widetilde{S}$ with respect to the Reynolds number, their ratio is thus constant. Nevertheless, from the expression of L_{-1} we expect that

$$\overline{L_{-1}}/\lambda_u \propto Re_d^{1/2} \propto R_\lambda, \tag{15}$$

where Re_d is the Reynolds number based on the local mean velocity defect and the cylinder diameter. In other words, the range of scales over which LI is satisfied progressively extends as the Reynolds number increases. The particular scale at which LI is expected to be observed depends on the magnitude of the coherent shear.

We now turn our attention to some possible persisting effect of local anisotropy in the far self similar region of the flow. Given $\mathscr{U}$ and $\mathscr{L}$ the similarity scales for which

$\mathscr{U} \propto x^{-1/2}$ and $\mathscr{L} \propto x^{1/2}$ the scaling of the turbulent strain rate is as follows

$$s(r) \propto \mathscr{U}/\mathscr{L} \propto x^{-1}. \tag{16}$$

For the sake of simplicity, the latter expressions do not consider explicitly the dependence on the virtual origin, x_0. This simply signifies that the turbulent strain rate acting at a given scale and the coherent strain rate decays at the same rate. Second, since

$$\overline{\langle\varepsilon\rangle} \propto \mathscr{U}^3/\mathscr{L} \propto x^{-2}, \tag{17}$$

$$\overline{\langle\lambda_u\rangle} \propto \mathscr{L} \propto x^{1/2}, \tag{18}$$

the anisotropic scale

$$\overline{L_{\tilde{S}}}/\lambda_u \propto x^0. \tag{19}$$

It is thus shown that from an initial anisotropic condition at the beginning of the self-similar region, the latter anisotropy persists independently of the downstream distance x. The degree of anisotropy depends on $\overline{S}+\widetilde{S}$ and therefore on initial conditions. Our results also support the proposition of George (1989) that there is no universal self-similarity but only local self-similarity conditioned by the topology and amplitude of the organized motion associated with each set of initial conditions.

CONCLUSIONS

An original LI test based on the ratio between the intensity of the turbulent strain rate and that due to the combined effect of the mean and coherent strain rates is proposed. This test is phenomenological and thus has an explicit dependence on the total large scale strain rate which induces anisotropy.

It has been shown that *(i)* when $\tilde{S}_\phi$ is important, LI only holds for scales smaller than the Taylor microscale *(ii)* when $\tilde{S}_\phi$ is small, the domain in which LI is valid extends up to the largest scales.

The analytical tool we have developed opens perspectives for a better understanding of the validity of LI in both decaying and shear flows, as a function of the dynamical behavior of large-scale statistics.

RAA acknowledges the support of the Australian Research Council. The financial support of the French National Research Agency (ANR) is gratefully acknowledged.

REFERENCES

Corrsin, S. 1958 Local isotropy in turbulent shear flow. *Tech. Rep.*. NACA RM.

Danaila, L., Antonia, R. A. & Burattini, P. 2012 Comparison between kinetic energy and passive scalar energy transfer in locally homogeneous isotropic turbulence. *Physica D* **241**, 224–231.

Durbin, P. A. & Speziale, C. G. 1991 Local anisotropy in strained turbulence at high Reynolds numbers. *Recent Advances in Mechanics of Structured Continua* **117**, 402–426.

George, W. K. 1989 The self preservation of turbulent flows and its relation to initial conditions and coherent structures. *Advances in Turbulence. Hemisphere, Editors W.K. George and R. Arndt.* pp. 1–41.

Hill, R.J. 2002 Exact second-order structure-function relationships. *J. Fluid Mech.* **468**, 317–326.

Hill, R. J. 2001 Equations relating structure functions of all orders. *J. Fluid Mech.* **434**, 379–388.

Kolmogorov, A. 1941 Dissipation of energy in the locally isotropic turbulence. *Dokl. Akad. Nauk. SSSR* **125**.

Monin, A. S. & Yaglom, A. M. 2007 *Statistical Fluid dynamics*, , vol. 2. MIT press.

Mouri, H. & Hori, A. 2010 Two-point velocity average of turbulence: Statistics and their implications. *Phys. Fluids* **22**, 115110.

O'Neil, J. & Meneveau, C. 1997 Subgrid-scale stresses and their modelling in a turbulent plane wake. *J. Fluid Mech.* **349**, 253–293.

Schumacher, J., Sreenivasan, K.R. & Yeung, P.K. 2003 Derivatives moments in turbulent shear flows. *Phys. Fluids* **15**, 84–90.

Thiesset, F., Danaila, L. & Antonia, R. A. 2013 Dynamical effect of the total strain induced by the coherent motion on local isotropy in a wake. *J. Fluid Mech.* **720**, 393–423.